

# Titanium dioxide in vanadate red phosphor compound for conventional white light emitting diodes

N. D. Q. ANH<sup>1</sup>, H. Y. LEE<sup>2,\*</sup>

<sup>1</sup>Faculty of Electrical and Electronics Engineering, Ton Duc Thang University, Ho Chi Minh City, Vietnam

<sup>2</sup>Department of Electrical Engineering, National Kaohsiung University of Sciences and Technology, Kaohsiung, Taiwan

The vanadate material  $\text{LiCa}_2\text{Mg}_2\text{V}_3\text{O}_{12}$  (LCMV) can serve as an excellent host matrix for the introduction of  $\text{Eu}^{3+}$  rare-earth ions as red luminescent centers to enhance the red emission component. To achieve this, we synthesized  $\text{Eu}^{3+}$ -doped LCMV phosphors using the conventional solid-state reaction route. The energy transfer mechanisms occurring between  $(\text{VO}_4)^{3-}$  groups and  $\text{Eu}^{3+}$  ions within the material were investigated with the emission decay curve calculation. We also integrated titanium dioxide ( $\text{TiO}_2$ ) nanoparticles with the prepared red phosphors and silicone gel, creating a color converter suitable for an LED lamp that emits warm white light. The light output of the LED was controlled by varying the concentration of  $\text{TiO}_2$  in the layer. The obtained results highlighted the potential of this vanadate-based red phosphor doping  $\text{TiO}_2$  composite as a promising converter for LED applications within the lighting and display sectors.

(Received December 6, 2023; accepted October 2, 2024)

**Keywords:** White LED, Red phosphor, Titanium dioxide, Color rendering index, Luminous efficacy

## 1. Introduction

The pursuit of inorganic phosphors with tunable luminescence has garnered significant attention due to their diverse applications, ranging from displays and light-emitting diodes to non-invasive thermometry [1–4]. Inorganic materials are the preferred luminescent hosts for introducing activators to achieve multicolor emissions. Among these, vanadate phosphors have emerged as standout candidates, offering exceptional optical performance with strong near-ultraviolet light absorption and comprehensive spectral luminescence [5–9]. Notably, certain vanadate phosphors, for instances  $\text{Ca}_5\text{Zn}_4(\text{VO}_4)_6$ ,  $\text{CsVO}_3$ , and  $\text{Ca}_2\text{KZn}_2\text{V}_3\text{O}_{12}$ , renowned for their self-activated luminescence properties, boasting broad emission and high quantum efficiency. However, the emission spectra of vanadate phosphors are relatively weak in red luminescence. Red-luminescence enhancement for vanadates can be achieved by doping rare-earth ions. The  $\text{Eu}^{3+}$  ion is a favorite rare-earth dopant to bolster the red emission component of phosphor hosts. It is worth noting that garnet-structured vanadate phosphors offer a versatile crystal lattice conducive to ionic substitution, leading to diverse chemical compositions. Crucially, this straightforward ionic substitution approach yields significant alterations in the luminescent properties of vanadate phosphors. This facile integration of  $(\text{VO}_4)^{3-}$  groups with  $\text{Eu}^{3+}$  ions facilitates color-tunable emissions, making it particularly valuable for applications in white light-emitting diodes.

The use of vanadate red phosphor prospectively improves the color rendering efficiency of the LED. However, the uniformity of light distribution outcome does not significantly benefit from just using red

phosphor. The scattering enhancement of the phosphor layer is supposed to regulate the transmitted light directions for a more even distribution. This idea can be conducted feasibly using the particles with great refractive index as a scatterer in the phosphor film. Among different particles such as  $\text{ZnO}$ ,  $\text{MgO}$ , and  $\text{SiO}_2$ , the  $\text{TiO}_2$  particle is extensively investigated due to its high index of refraction, excellent stability, high transmission under visible and near-infrared excitation sources, and non-toxicity. Additionally, conventional  $\text{TiO}_2$  particles offer high scattering efficiency across the entire visible spectrum, stability, and versatile application capabilities [11,12].

In our study,  $\text{LiCa}_2\text{Mg}_2\text{V}_3\text{O}_{12}$  (LCMV) vanadate materials provided an excellent matrix for doping rare-earth ions, such as  $\text{Eu}^{3+}$ , to serve as red luminescent centers and enhance the red emission component. We successfully synthesized  $\text{Eu}^{3+}$ -doped LCMV phosphors (LCMV:Eu) exhibiting multicolor luminescence through the conventional solid-state reaction route. Our investigation delved into the emission and energy transfers between  $(\text{VO}_4)^{3-}$  groups and  $\text{Eu}^{3+}$  ions. Subsequently, we integrated  $\text{TiO}_2$  nanoparticles with the prepared red phosphors and silicone gel to create a color converter ( $\text{TiO}_2@\text{LCMV:Eu}$ ) for an LED lamp, yielding warm white light. The control over light output of the LED was facilitated by varying the concentration of  $\text{TiO}_2$  in the layer. The results were shown and discussed in the next sections, indicating that the  $\text{TiO}_2$ -integrated vanadate-based red phosphor compound can serve as a promising converter for LED application in the lighting and display fields.

## 2. Method

The LCMV:Eu red phosphors were produced with the solid-phase reacting method. The starting components include  $\text{Eu}_2\text{O}_3$ ,  $\text{CaCO}_3$ ,  $\text{Li}_2\text{CO}_3$ ,  $\text{NH}_4\text{VO}$ , and  $\text{MgO}$ . The doping amount of  $\text{Eu}^{3+}$  was determined at 0.01. All these components were weighed and mixed by grinding with ethanol. Next, the mixture was subjected to a crucible and proceeded to an 800-degree Celsius sintering lasting 4 hours. The obtained product was then calcinated, followed by powdering for examinations. For collecting the emission and excitation spectra and emission decay curves of the phosphors, we used the Edinburgh FS5 spectrofluorometer utilizing an excitation source of 150-W xenon lamps.

The LED used in this work was prepared with a near-ultraviolet chip (360 nm), the  $\text{TiO}_2@\text{LCMV:Eu}$  red phosphor layer,  $\text{YAG:Ce}^{3+}$  yellow phosphor, and blue-phosphor  $\text{Eu}^{2+}$ -integrated  $\text{BaMgAl}_{10}\text{O}_{17}$ . The concentration of  $\text{TiO}_2$  changes from 5-50 wt%, while that of the red and blue phosphor components were fixed. Besides, when increasing the  $\text{TiO}_2$  concentration, the integrating amount of yellow phosphor  $\text{YAG:Ce}^{3+}$  has to be reduced to maintain the correlated color temperature (CCT) of the prepared LED device, see Fig. 1. For the characterization of the LED's luminosity, we applied an integrating sphere.

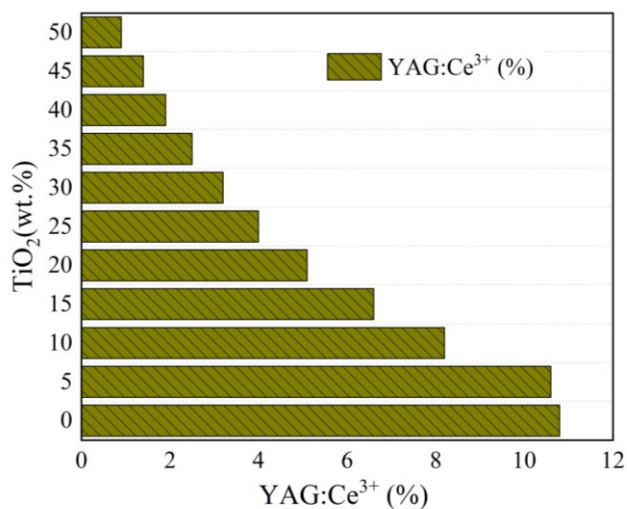


Fig. 1. Reducing the  $\text{YAG:Ce}^{3+}$  concentration with increasing  $\text{TiO}_2$  amount in the phosphor compound

## 3. Computation and discussion

When subjected to excitation at 360 nm, in addition to the characteristic  $(\text{VO}_4)^{3-}$  emission, the prepared LCMV:Eu phosphors also exhibited the distinct transition emissions of  $\text{Eu}^{3+}$  ions ( $^5\text{D}_0 \rightarrow ^7\text{F}_J$ ,  $J=1, 2, 3, 4$ ). Notably, the dominance of the  $\text{Eu}^{3+}$  transition from  $^5\text{D}_0$  to  $^7\text{F}_2$  emission occurred specifically when  $\text{Eu}^{3+}$  ions occupied lattice sites lacking inversion symmetry [21]. This demonstrated the substitution of  $\text{Ca}^{2+}$  ions by  $\text{Eu}^{3+}$  ions in the LCMV:Eu phosphors. Upon monitoring at 610 nm, a sharp peak at

395 nm emerged, attributed to the  $\text{Eu}^{3+}$  transition from  $^7\text{F}_0$  to  $^5\text{L}_6$ . Under the emission wavelengths of 610 nm and 520 nm, the excitation wavelengths showed an overlap, suggesting that the  $\text{Eu}^{3+}$  emission may originate from  $(\text{VO}_4)^{3-}$  groups through energy transfer mechanisms. The emission decay curves of the phosphor can be a useful means to demonstrate such energy transfer mechanisms, using the following equations:

$$I_T = I_0 + C_1 \exp(-t/\tau_1) + C_2 \exp(-t/\tau_2) \quad (1)$$

$$\tau = \frac{C_1 \times (\tau_1)^2 + C_2 \times (\tau_2)^2}{C_1 \times \tau_1 + C_2 \times \tau_2} \quad (2)$$

where the  $\tau_1$  is the short, and  $\tau_2$  is the long lifetimes, while  $C_1$  and  $C_2$  are constant values. The emission intensity is denoted by  $I$ , and  $t$  is the time. The emission decay curves exhibited an excellent fit using the aforementioned bi-exponential equation, indicating the presence of two distinct luminescence centers. These centers are likely associated with the  $^3\text{T}_2 \rightarrow ^1\text{A}_1$  and  $^3\text{T}_1 \rightarrow ^1\text{A}_1$  transitions within the  $(\text{VO}_4)^{3-}$  groups. Notably, as the concentration of  $\text{Eu}^{3+}$  increased, the  $\tau$  value decreased, providing compelling evidence of energy transfer from  $(\text{VO}_4)^{3-}$  groups to  $\text{Eu}^{3+}$  ions.

When the LCMV:Eu was coupled with other materials to make a white LED module, the red emission originating from  $\text{Eu}^{3+}$  ions was significant to compensate for the red-light deficiency in the total spectra of the LED. The emission power of the LED built with  $\text{TiO}_2@\text{LCMV:Eu}$  layer and other phosphor materials is shown in Fig. 2. The changes in emission shape and intensity are monitored by varying  $\text{TiO}_2$  integrating concentrations.

Overall, the emission spectra of the LED shows two distinct ranges, including a broad 500-600 nm band and a narrower band of  $\sim 450$ -465 nm. The emission peaks are noted at 460 nm, 540 nm, and  $\sim 590$  nm, occurring from phosphor components in the packages. At first, when the concentration of  $\text{TiO}_2$  changes from 0-15wt%, the emission shape does not change but its intensity. Specifically, the intensity of the emission declined while the emission peaks' positions remained the same on the increasing  $\text{TiO}_2$  concentration. However, further increasing the  $\text{TiO}_2$  amount, both the intensity and positions of emission peaks change. The reduction in intensity of the LED emission is notable when  $\text{TiO}_2$  increases in concentration, from 20wt% to 50 wt%. Additionally, the emission peak at 520 nm is recorded with more than 20 wt% of  $\text{TiO}_2$  in the  $\text{TiO}_2@\text{LCMV:Eu}$  layer, which can originate from the LCMV:Eu phosphor base. Meanwhile, the emission peak at 460 nm is gradually diminished.

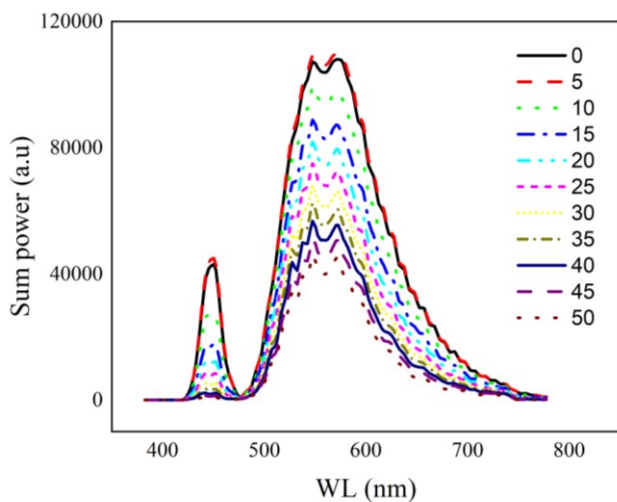


Fig. 2. Changes in emission of LED with varying  $\text{TiO}_2$  amount in the phosphor compound (color online)

The changes in LED total emission power can be induced by the internal scattering performance. As  $\text{TiO}_2$  was reported to be a notable scattering-enhancement particle, it is expected that increasing  $\text{TiO}_2$  concentration results in stronger scattering in the LED model. The reduced scattering coefficients with  $\text{TiO}_2$  concentration ranging from 5–50 wt% are in Fig. 3. Across the visible light range, 400–680 nm, the higher the concentration of  $\text{TiO}_2$ , the greater the reduced scattering coefficients. Such findings indicate the probability of higher blue-light absorption and conversion in the package, which demonstrates the diminishing blue emission peak in Fig. 2, when increasing  $\text{TiO}_2$  contents. Though the higher scattering performance induces the better color conversion of red-phosphor film for the improvement of uniform color distribution, the decreasing intensity of the whole emission range can affect the lumen output of the LED. In Fig. 4, the lumen output of the LED declines in intensity when we continuously increase the  $\text{TiO}_2$  concentration. However, at the lowest concentration value of  $\text{TiO}_2$ , 5 wt%, we notice a slight increase in the lumen output. So, a small amount of 5 wt%  $\text{TiO}_2$  in the phosphor compound can be useful for enhancing the lumen intensity of the fabricated LED while elevating the scattering productivity.

The stronger scattering can support to achievement of a more uniform color dispersion, enhancing the chroma uniformity of the generated white light. In other words, to obtain higher color uniformity, the chroma deviation (or delta CCT) needs to be hindered, and better scattering performance can help. The chroma deviation of the LED is shown in Fig. 5 and is supported by the angular-CCT values in Fig. 6.

With the increase in  $\text{TiO}_2$  concentration, the delta CCT values significantly, attributed to the absorption and scattering effects of the phosphor materials. The color deviation is notable when we use the  $\text{TiO}_2$  amount at 25 wt% and 30 wt%, with the value at 25 wt%  $\text{TiO}_2$  being the highest. Compared to the reference value (0 wt%  $\text{TiO}_2$ ), the delta-CCT levels at 15 and 45 wt%  $\text{TiO}_2$  contents are noticeably lower. Notably, the delta CCT with 45 wt% of  $\text{TiO}_2$  is the lowest. The angular CCT in Fig. 6 shows such fluctuation, aligned with the results in Fig. 5. Moreover, based on the collected angular CCTs, the presence of  $\text{TiO}_2@LCMV:\text{Eu}$  compound contributes to achieving the warm white light in the CCT range of around 3900–4075 K.

The better color uniformity can also be attributed to the angle-dependent scattering of the  $\text{TiO}_2$ . Specifically, this can be discussed via the angular dependent CCT range in Fig. 6, combined with data in Fig. 3. When being under the ultraviolet (380 nm) region, the scattering of  $\text{TiO}_2$  is often in the forward direction. The longer wavelengths in the visible range broaden the scattering angle, leading to a higher reduced scattering efficiency in the layer. Additionally, the greater amount of  $\text{TiO}_2$  in the compound contributes to a widened scattering angle as the light contacts more with the particles in the film when the space between particles is less. In other words, the scattering is in all directions with the higher percentage of  $\text{TiO}_2$  in the phosphor compound. As a result, the color deviation is prospectively minimized for better color uniformity output [22].

In addition to the color-distribution homogeneity, we also examined the rendering efficiency of the LED light on the introduction of  $\text{TiO}_2@LCMV:\text{Eu}$  compound. The color rendering index and color quality scale, shortened as CRI and CQS hereafter, are critical parameters in our work. The color quality scale holds significant importance as a comprehensive metric for evaluating color reproduction, surpassing the constraints associated with the traditional color rendering index. Unlike CRI, the CQS accounts for a diverse set of factors, including hue preservation, chroma enhancement, gamut area index, and gamut shape index [23, 24]. This comprehensive approach provides a nuanced and thorough evaluation of a light source's color performance, rendering it an invaluable tool for optimization in various applications.

In Fig. 7, the CQS declines drastically with heightened  $\text{TiO}_2$  concentration. This phenomenon is also observed in the case of CRI in Fig. 8. Nevertheless, at 5 wt% of  $\text{TiO}_2$ , we observed similar CQS and CRI levels to the reference values. From the obtained findings, 5 wt% of  $\text{TiO}_2$  can be a good concentration for the  $\text{TiO}_2@LCMV:\text{Eu}$  compound to improve the LED luminosity and preserve the rendering performance. Meanwhile, to accomplish the better color distribution, 45 wt% of  $\text{TiO}_2$  turns out to be the most suitable choice.

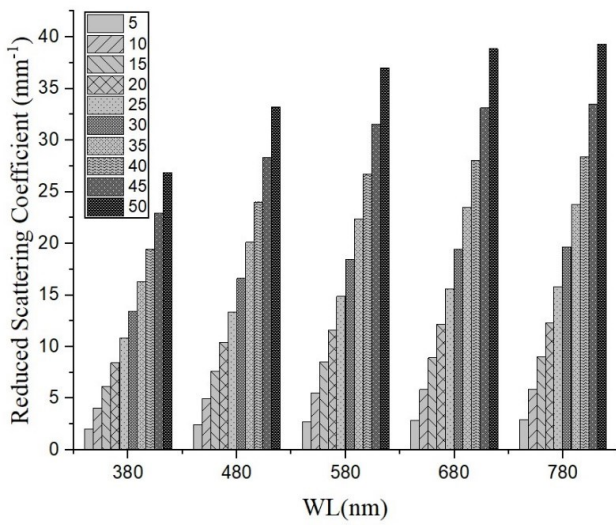


Fig. 3. Reduced scattering coefficient values with varying TiO<sub>2</sub> amount in the phosphor compound

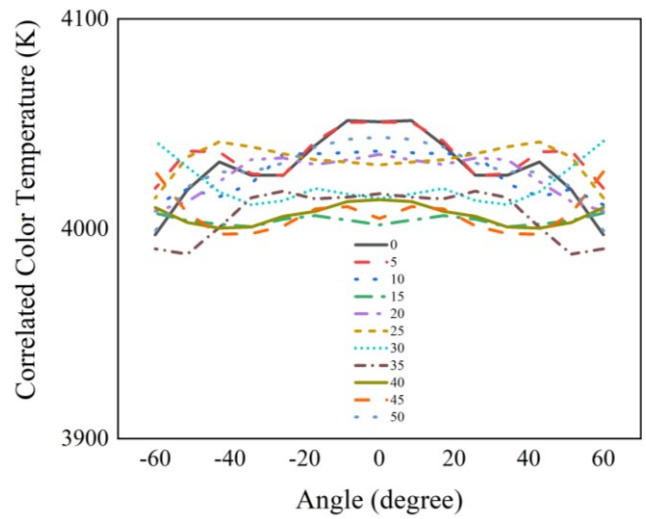


Fig. 6. Angular CCT of the prepared LED with varying TiO<sub>2</sub> amount in the phosphor compound (color online)

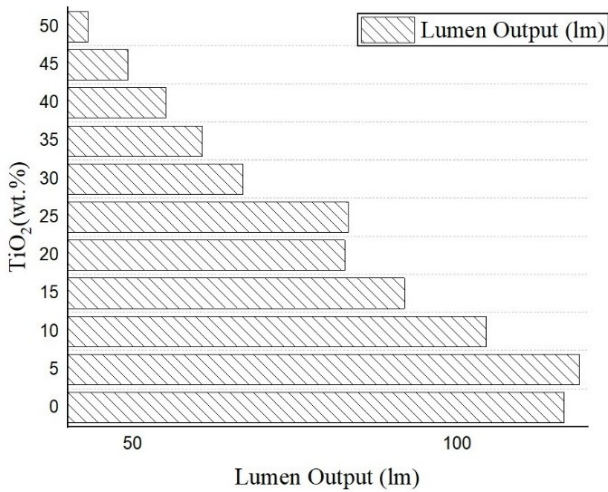


Fig. 4. Lumen output of the prepared LED with varying TiO<sub>2</sub> amount in the phosphor compound

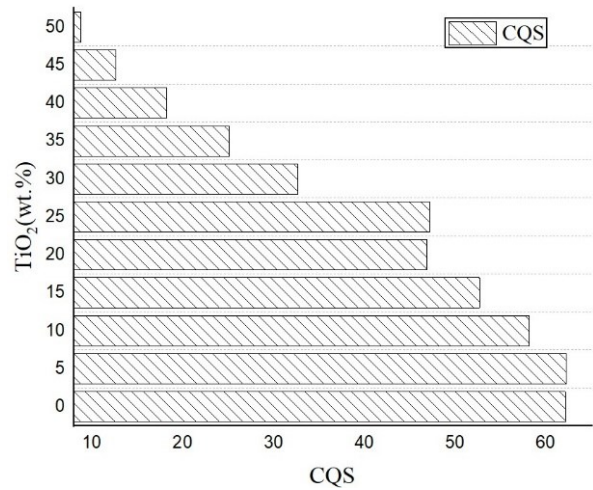


Fig. 7. Color quality scale of the prepared LED with varying TiO<sub>2</sub> amount in the phosphor compound

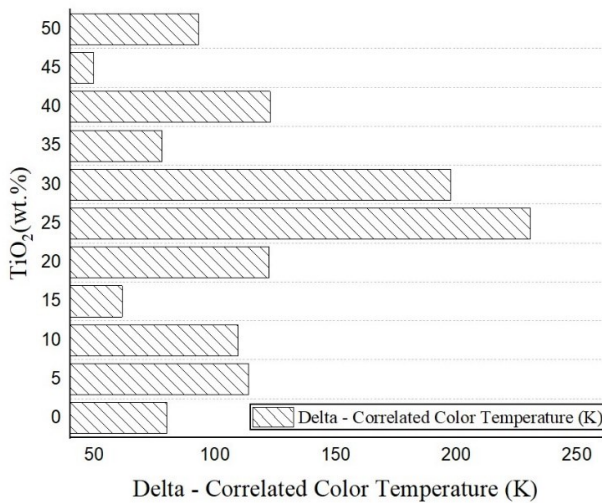


Fig. 5. Delta CCT of the prepared LED with varying TiO<sub>2</sub> amount in the phosphor compound

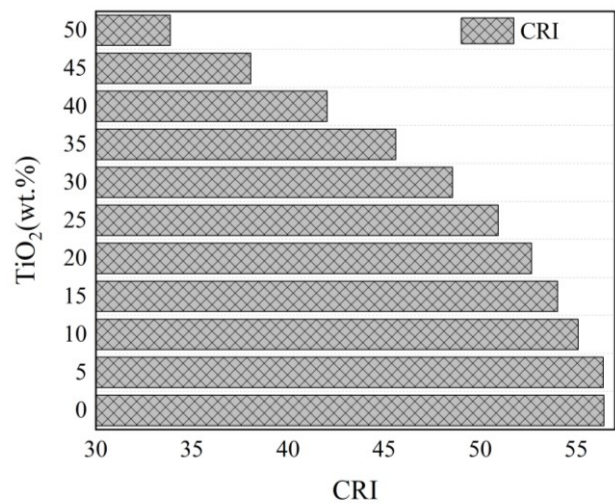


Fig. 8. Color rendering index of the prepared LED with varying TiO<sub>2</sub> amount in the phosphor compound

#### 4. Conclusions

In this paper, the  $\text{TiO}_2@\text{LCMV:Eu}$  red-phosphor compound was used to fabricate the LED model. The performance of LED packages was controlled with varying  $\text{TiO}_2$  concentration. The scattering performance was facilitated by increasing  $\text{TiO}_2$  concentrations. The color uniformity can be improved with the enhanced scattering efficiency, while the luminosity could decline owing to high light re-absorption. From the obtained findings, 5 wt% of  $\text{TiO}_2$  can be a good concentration for the  $\text{TiO}_2@\text{LCMV:Eu}$  compound to improve the LED luminosity and preserve the rendering performance. Meanwhile, to accomplish better color distribution, 45 wt% of  $\text{TiO}_2$  turns out to be the most suitable choice. Thus, the  $\text{TiO}_2@\text{LCMV:Eu}$  compound can become a potential material for near-ultraviolet-pumped white LED devices. Further modifications on the  $\text{TiO}_2@\text{LCMV:Eu}$  compound will be critical to extend its application.

#### References

- [1] X. Huang, X. Zhao, Z. C. Yu, Y. C. Liu, A. Y. Wang, X.-J. Wang, F. Liu, *Opt. Mater. Express* **10**, 1163 (2020).
- [2] H. S. El-Ghoroury, Y. Nakajima, M. Yeh, E. Liang, C.-L. Chuang, J. C. Chen, *Opt. Express* **28**, 1206 (2020).
- [3] N. D. Q. Anh, P. X. Le, H. -Y. Lee, *Curr. Opt. Photon.* **3**, 78 (2019).
- [4] Q. Xu, L. J. Meng, X. H. Wang, *Appl. Opt.* **58**, 7649 (2019).
- [5] S. Pan, B. Yang, X. R. Xie, Z. X. Yun, *Appl. Opt.* **58**, 2183 (2019).
- [6] Q. Zhang, R. L. Zheng, J. Y. Ding, W. Wei, *Opt. Lett.* **43**, 3566 (2018).
- [7] T. P. White, E. Deleporte, T.-C. Sum, *Opt. Express* **26**, A153 (2018).
- [8] A. Ullah, Y. Zhang, Z. Iqbal, Y. Zhang, D. Wang, J. Chen, P. Hu, Z. Chen, M. Huang, *Biomed. Opt. Express* **9**, 1006 (2018).
- [9] A. Lihachev, I. Lihacova, E. V. Plorina, M. Lange, A. Derjabo, J. Spigulis, *Opt. Express* **9**, 1852 (2018).
- [10] A. Kho, V. J. Srinivasan, *Opt. Lett.* **44**, 775 (2019).
- [11] J.-S. Li, Y. Tang, Z.-T. Li, L.-S. Rao, X.-R. Ding, B.-H. Yu, *Photon. Res.* **6**, 1107 (2018).
- [12] C. Zhang, B. Yang, J. Chen, D. Wang, Y. Zhang, S. Li, X. Dai, S. Zhang, M. Lu, *Opt. Express* **28**, 194 (2020).
- [13] H. Jia, Q. J. Wu, C. Jiang, H. Wang, L. Q. Wang, J. Z. Jiang, D. X. Zhang, *Appl. Opt.* **58**, 704 (2019).
- [14] Y. Shi, S. Ye, J. Yu, H. Liao, J. Liu, D. Wang, *Opt. Express* **27**, 38159 (2019).
- [15] X. Yang, C. F. Chai, J. C. Chen, S. S. Zheng, C. Chen, *Opt. Mater. Express* **9**, 4273 (2019).
- [16] S.-R. Chung, C.-B. Siao, K.-W. Wang, *Opt. Mater. Express* **8**, 2677 (2018).
- [17] S. C. Song, X. L. Ma, M. B. Pu, X. Li, Y. H. Guo, P. Gao, X. G. Luo, *Photon. Res.* **6**, 492 (2018).
- [18] J. H. Park, I. J. Ko, G. W. Kim, H. Lee, S. H. Jeong, J. Y. Lee, R. Lampande, J. H. Kwon, *Opt. Express* **27**, 25531 (2019).
- [19] J. Hao, H.-L. Ke, L. Jing, Q. Sun, R.-T. Sun, *Appl. Opt.* **58**, 1855 (2019).
- [20] C. Polzer, S. Ness, M. Mohseni, T. Kellerer, M. Hilleringmann, J. Rädler, T. Hellerer, *Biomed. Opt. Express* **10**, 4516 (2019).
- [21] H. Lee, S. Kim, J. Heo, W. J. Chung, *Opt. Lett.* **43**, 627 (2018).
- [22] L. T. T. My, N. L. Thai, T. M. Bui, H.-Y. Lee, N. D. Q. Anh, *Materials Science Poland* **40**, 105 (2022).
- [23] H. T. Tung, D. A. N. Thi, N. D. Q. Anh, *Bulletin of Electrical Engineering and Informatics* **12**, 3388 (2023).
- [24] H. T. Tung, M. H. N. Thi, N. D. Q. Anh, *International Journal of Technology*, **15**, 8 (2024).

\*Corresponding author: lechy@nkust.edu.tw;  
nguyendoanquocanh@tdtu.edu.vn